Biosensors and Bioelectronics 141 (2019) 111430

Contents lists available at ScienceDirect

Biosensors and Bioelectronics

journal homepage: www.elsevier.com/locate/bios

Real-time bacterial detection with an intracellular ROS sensing platform

J.M. Hicks[a], R. Halkerston[b], N. Silman[b], S.K. Jackson[c], J.W. Aylott[a], F.J. Rawson[a,*]

[a] Regenerative Medicine and Cellular Therapies, University of Nottingham, Nottingham, UK
[b] Public Health England, Porton Down, UK
[c] Medicine and Dentistry, University of Plymouth, Plymouth, UK

ARTICLE INFO

Keywords:
ROS
Bacteria
Hydrogen peroxide
SWCNT
Biosensor
Macrophage

ABSTRACT

Reactive oxygen species are highly reactive molecules that as well as being ubiquitously expressed throughout the body, are also known to be involved in many diseases and disorders including bacterial infection. Current technology has limited success in the accurate detection and identification of specific reactive oxygen species. To combat this, we have developed an electrochemical biosensor that is constructed from single walled carbon nanotubes that have been immobilised on an indium tin oxide surface functionalised with osmium-based compound. This sensor was integrated within mouse macrophage cells (RAW 264.7) with multiple serotypes of bacteria used to initiate an immune response. Intracellular hydrogen peroxide was then measured in response to the interaction of the lipopolysaccharides, present on the outer wall of Gram-negative bacteria, with the Toll-like Receptor 4. Additional controls of n-acetylcysteine and sodium pyruvate were implemented to prove the specificity of the sensor towards hydrogen peroxide. The sensors were found to have a lower limit of detection of 368 nM hydrogen peroxide. An increase in intracellular hydrogen peroxide was detected within 3 seconds of interaction of the bacteria with the macrophage cells. This low limit of detection combined with the rapid response of the sensor resulted in the unprecedented detection of hydrogen peroxide on a temporal level not previously seen in response to a bacterial threat. From the three serotypes of Gram-negative bacteria that were tested, there were distinct differences in hydrogen peroxide production. This proves that the innate immune system has the ability to respond dynamically and rapidly, after infection prior to the activation of the adaptive immune system.

1. Introduction

Reactive oxygen species (ROS) are a class of molecules that are typically derived from oxygen metabolism. Apart from hydrogen peroxide and hydroxide ions, ROS are all radicals with an unpaired electron in their outer shell. This makes ROS highly reactive and able to act as rapid oxidisers of various target proteins. ROS are ubiquitously expressed in a strictly controlled manner and play diverse roles in biology that are dictated by their concentration and location. Other than their roles in normal cellular function, ROS play intricate roles in various diseases and inflammation where they are upregulated. ROS are known to be involved in many different diseases including Parkinson's, arthritis, inflammation and sepsis (Mateen et al., 2016; Hwang, 2013; Mittal et al., 2014; Oliveira et al., 2017). The concentration of ROS within a cell can determine whether the cell divides and grows normally (Schulze-Osthoff et al., 1995) or triggers apoptosis. For example, it has been shown that hydrogen peroxide at concentrations of less than 0.7 μM supports proliferation, apoptosis is triggered between 1 and 3 μM and concentrations of more than 3 μM causes cellular necrosis (Lennicke et al., 2015). Due to the diverse roles of ROS in both cell life and death, they are an important topic of study; however, due to their high reactivity and transient nature, measurement is extremely difficult.

ROS are produced within immune cells in response to bacterial infection. Lipopolysaccharides (LPS) embedded on the outer membrane of Gram-negative bacteria, interact with the Toll-like receptor 4 (TLR4) (Salomao et al., 2008) present on many cell types, including macrophages. TLR4 has multiple intracellular signalling domains which are recruited upon activation. A key signalling domain for ROS production is myeloid differentiation factor-88 (MyD88). MyD88 is then responsible for the association of interleukin-1R-associated kinase-4 (IRAK-4) to TLR4. Upon association IRAK-4 is auto-phosphorylated and leaves the TLR4/MyD88 complex to interact with tumour necrosis factor receptor-associated factor 6 (TRAF6)(Akira and Hoshino, 2003). It is this interaction that is key in the production of ROS. The interaction between IRAK4 and TRAF6 can activate both NF-κB (Ryan et al.,

* Corresponding author.
E-mail address: frankie.rawson@nottingham.ac.uk (F.J. Rawson).

https://doi.org/10.1016/j.bios.2019.111430
Received 4 April 2019; Received in revised form 23 May 2019; Accepted 7 June 2019
Available online 19 June 2019

2004; Asehnoune et al., 2004), and the MAPK pathways (Matsukawa et al., 2004) as well as, importantly, activating another membrane bound protein: NADPH oxidase (NOX), through the phosphorylation of one of NOXs intracellular subunits (Pacquelet et al., 2007; Brandes et al., 2014). The NOX family of proteins produces superoxide radicals through the oxidation of NADP to NADPH and the co-reduction of oxygen to superoxide. Superoxide then in turn forms hydrogen peroxide (Lennicke et al., 2015). Which signalling pathway that is activated is thought to be dependent on the ROS generated in a temporally dependent manner (Terada, 2006). For example, prolonged and diffused, production of ROS is thought to be a trigger for cells activating apoptotic pathways through non-specific oxidative damage (Terada, 2006). The two major classes of LPS are smooth (wild type, WT) and rough LPS. Rough LPS is truncated in length when compared to smooth and bypasses the cells escort system to TLR4 often resulting in a larger ROS response. The variety of outcomes possible from this one interaction of LPS with TLR4 may explain how the innate immune system can react differently to different bacterial serotypes. Developing a technique for the accurate detection of ROS is vital in elucidating the role they play in the innate immune system.

An ideal technique for ROS detection therefore, needs to have the ability to selectively sense intracellular ROS in a time sensitive manner. The technique should also be relatively cheap and easy to construct in order to be commercialised. Measurements should be easy to obtain without requiring extra, specialist equipment. Such a technique does not currently exist though there is a vast library of methods that can be used to some extent.

For many years fluorescent probes have been the fore-runner in ROS detection as they are widely available and have decades of papers behind them. While their commercial availability is important for user access, they have many benefits and drawbacks which have been reviewed thoroughly by Gomes and Winterbourn (Gomes et al., 2005; Winterbourn, 2014).

Electrochemical based sensors have been around since the early 1950's (Leland et al., 1953; Clark and Clark, 1987) and are quickly becoming a competitor to the traditional fluorescent probe. Electrochemical sensors are based on a recognition element for specificity and a transducer that converts a biological event to an electrical signal (such as change in concentration converted to a change in current). This transducer element allows for a rapid detection system that is not dependent on chemical reactions or incubation periods like many traditional methods are. The adaptability of the recognition element also allows for specificity to the analyte of interest. These components of electrochemical sensors when combined with their small size (nano to micro scale) makes them an extremely advantageous detection method for intracellular and extracellular analytes. Due their diverse applications and extreme adaptability, many electrochemical sensors have been developed for the detection of biologically relevant compounds often using the presence of hydrogen peroxide as an indicator for a different analyte of interest. It is only in recent years that the technology has been adapted for the direct detection of intracellular ROS. Amperometric electrochemical biosensors which measure a change in current directly proportional to the concentration of the analyte of interest (Kotanen et al., 2012), are particularly common (Grieshaber et al., 2008; Belluzo et al., 2008).

The first step in investigating the role of ROS in the immune system is the development of a sensor that can specifically detect and distinguish one member of the ROS family. In this work we present the further development of an intracellular biosensor that can detect hydrogen peroxide in a concentration and time dependent manner, in response to bacterial interrogation, and this builds on our previous work in developing the sensing platform (Rawson et al., 2011, 2013, 2015). We construct an amperometric sensor utilising single walled carbon nanotubes (SWCNTs) that were modified with an osmium-based electrocatalyst that mimics catalase behaviour (Rawson et al., 2011). We have previously demonstrated that sensors can be inserted inside of cells

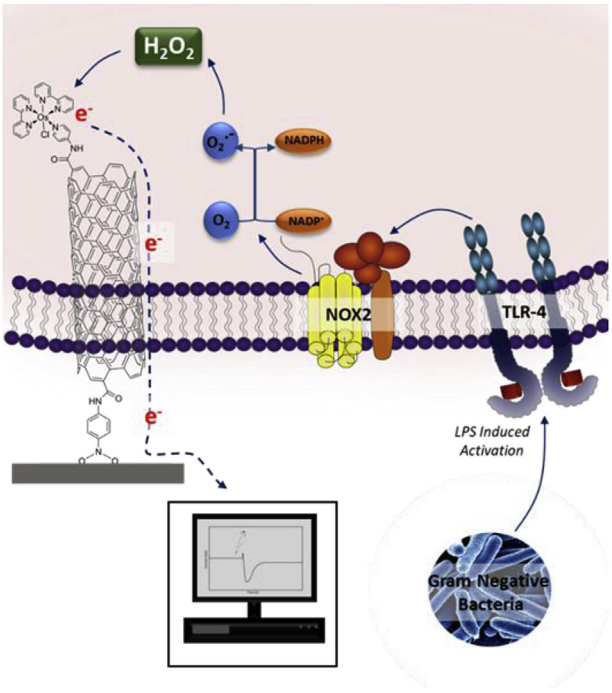

Fig. 1. Schematic of the interface between CNT biosensor and mammalian macrophage cells (RAW 264.7), highlighting the biological pathway of interest. In brief LPS from gram negative bacteria activates TLR-4 which then triggers the production of intracellular reactive oxygen species which can be detected though electron exchange with the CNT and detected.

(Rawson. et al., 2013, 2015). These sensors (ITO-SWCNTs-Osby) were then used to investigate the distinct hydrogen peroxide response rapidly produced within macrophage cells when exposed to a LPS isolated from bacteria. An overview of how bacteria induce hydrogen peroxide within the cell, and how it is detected by the amperometric biosensor is shown in Fig. 1. The detailed electrocatalytic mechanism which results in hydrogen peroxide detection can be found in our recent publication (Rawson et al., 2015).

The osmium core of the sensor can be maintained in either its oxidised or reduced form dependant on what potential is being applied. Hydrogen peroxide can then oxidise or reduce the osmium, the re-reduction/re-oxidation of the osmium by the maintained potential is then measured and detected as a change in current proportional to the concentration of hydrogen peroxide. Therefore, the osmium compound acts as a catalase mimic and the mechanism of sensing and origin of LPS induced ROS production has been extensively discussed in our previous report (Rawson et al., 2015).

Using this amperometric biosensor, any change in intracellular hydrogen peroxide concentration will be detected through the combined use of the osmium (Osby) based recognition element and the carbon nanotube transducer. The application of this biosensor to investigate the hydrogen peroxide response to Gram-negative bacterial infection will provide valuable insight to the dynamic processes activated from activation to bacterial response. We hypothesise that different bacteria will result in different hydrogen peroxide responses within macrophage cells. This change in concentration could then theoretically be used to identify the infection when unknown. Before this can be investigated, however, it is important to determine what differences, if any, there are in hydrogen peroxide production in response to infection. This will be explored through the use of three different bacterial serotypes: *E.coli* (0111:B4, WT), *S.minnesota* (WT) and *S.minnesota* (Re595).

2. Experimental

2.1. Materials and reagents

Unless otherwise stated all materials were obtained from Sigma-Aldrich.

2.2. Electrochemical studies

All electrochemical studies were conducted using a Metrohm Multi Autolab multichannel potentiostat. A standard three electrode system was used with the working electrode constructed as described, a silver/silver chloride reference electrode and a platinum wire counter electrode (ALS Co. Ltd). The ITO-SWCNT-Osby sensor acts as the working electrode. The ITO was obtained from Delta Technologies Ltd and the SWCNTs were purchased from Nanolab Inc.

2.3. Osmium synthesis

Osmium (II)bis-2,2-bipyridine (p-aminomethyl pyridine)chlorido hexafluorophosphate was synthesised as described previously (Rawson et al., 2011).

2.4. Osmium binding

ITO-SWCNTs were coupled to the Osmium (II)bis-2,2-bipyridine (p-aminomethyl pyridine)chlorido hexafluorophosphate (Osby) complex through the exposed carboxylic groups on the SWCNTs. SWCNTs were immersed in a mixed solution of 40 mM 1-ethyl-3-(3-dimethyl aminopropyl) carbodiimide hydrochloride (EDC) and 10 mM N-hydroxysuccinimide (NHS) in MilliQ water for 1 hour before transferring the SWCNTs to a 2.5 mM solution of the $Os(bpy)_2Cl$ (4-aminomethyl pyridine)+ that had been solubilised in a mix solution of PBS and ethanol (7:3) for 24 hours.

2.5. Sensor construction

Sensors were constructed as described previously (Hicks et al., 2017; Rawson et al., 2015). Briefly, an indium tin oxide (ITO, Delta Technologies Ltd.) surface was modified with a poly-phenylamine layer formed from the electrografting (10 s, −0.6 V) of an *in situ* formed diazonium compound. Single walled carbon nanotubes (SWCNT's, Nanolab Inc.) were tethered to this layer via EDC/NHS chemistry and further modified with an osmium complex (osmium (II)bis-2,2-bypyridine (p-aminomethylpyridine)chlorido hexafluorophosphate; Osby). Sensors were electrochemically tested for stability prior to use by performing cyclic voltammetry (100 scans, 0.1 Vs^{-1}, 0 V to −0.6 V) in PBS (10 mM) with an Ag/AgCl reference electrode and a platinum counter electrode. The final sensor construct is abbreviated to ITO-SWCNT-Osby.

2.6. Hydrogen peroxide calibration

Calibration of the sensors and calculation of the limit of detection was performed with chronoamperometry. A fixed potential of 0.15 V was applied to facilitate the reduction of the osmium compound tethered to the SWCNTs, with an interval time of 0.1 s. Hydrogen peroxide was serially diluted in 10 mM PBS to a range of concentrations from 0 μM (PBS only) to 80 μM. Chronoamperometric experiments were performed on solutions that varied in concentration for 150s. The final 10 data points (1s) were averaged to calculate the mean current for that concentration of hydrogen peroxide. This was then subtracted from the PBS control which results in the mean reduction current facilitated by the hydrogen peroxide. This was plotted versus concentration and the linear portion of the graph was used for the calculation of the limit of detection.

2.7. Cell culture

RAW 264.7 cells were obtained from ECACC and were cultured in T80 flasks (Nunclon) in 20 ml of culture media (DMEM, high glucose, 10% FBS, 2.5% HEPES) in an incubator at 37 °C and 5% CO_2. Cells were grown to 80% confluency before being harvested with a cell scraper (Corning). When used in hydrogen peroxide assay (see below) cells were either left untreated or treated for 2 hours with either 10 mM NAC, 10 mM sodium pyruvate or 1 μM TAK-242 (Cayman Chemical).

2.8. Bacterial culture

E. coli (0111:B4) and *S. minnesota* (WT) were obtained from Public Health England's NCTC culture collection. *S. minnesota* (Re595) was obtained from the ATCC. Stock cultures of bacterium were created by growing bacteria on streaked TSA plates (trypticase soy agar, Oxoid) overnight. Bacterial colonies were then harvested and suspended and grown in broth (LB was used for the *E. coli* culture and TSB for both *S. minnesota* strains) until an absorbance at 600 nm of 0.5 was achieved. (Typically 1–2 hours). Cultures were then diluted with glycerol (25% final concentration) and aliquoted and frozen at −80 °C until use. Glycerol stocks were thawed to room temperature and used to streak plates the day before experiments and stored in an incubator at 37 °C and 5% CO_2 (Brunswick Galaxy 170s incubator). On the day of experiments bacterial colonies were harvested from plates and grown in broth in 250 ml baffled flasks (Thermofisher) in a shaking incubator (Stuart orbital incubator S1500) at 37 °C for the desired amount of time. Growth was tracked by measuring the absorbance at 600 nm (OD_{600}) using a spectrophotometer (WPA Biowave II).

2.9. LAL assay

Lipopolysaccharide (LPS) concentration was calculated using the commercial LAL chromogenic endpoint assay kit from Hycult Biotech (HIT302) which measure endotoxin units per ml (12 EU/ml ~ 1 ng/ml LPS). Bacteria were grown as described for two hours and diluted 1:1000 prior to use in the assay. A set of standards (provided by the supplier) was tested on every plate with additional controls of just the broth (LB or TSB, diluted 1:1000) with and without the LAL reagent. Endotoxin free water was used for all the dilutions. The LAL reagent binds to endotoxins producing a yellow colour. Absorbance at 405 nm was measured using a VERSAmax tuneable microplate reader (BN02863).

2.10. Hydrogen peroxide detection

ITO-CNT-Osby sensors were placed within a 12 well plate (Corning). Cells were harvested from the T80 flasks and counted using an automated counter (Invitrogen countess); 0.5×10^6 cells were then gently pipetted onto each sensor and inserted onto the CNTs via centrifugation (Sorvail Legend RT) at 1000 rpm for 3 minutes. Sensors were rinsed in sterile PBS (Severn Biotech) to remove excess cells. The sensors (+cells) as the working electrode were assembled with the rest of the electrochemical cell so that a circle of 3 mm in diameter was exposed to the electrolyte (800 μL sterile 1 × PBS) and the exposed portion of the sensor was dried with argon gas. A fixed potential of 0.15 V (vs Ag/AgCl) was applied. Simultaneously, bacteria that had been growing in suspension for 2 hours previously, was centrifuged at 3060 G for 5 minutes to form a pellet of the bacteria. Bacteria was then re-suspended in sterile PBS to a final concentration of 500 ng/ml of LPS (calculated from LAL assay). 200 μL of bacterial suspension was pipetted into the analyte (termed time '0', final concentration 100 ng/ml) and the change in current was measured for 5 minutes post-infection.

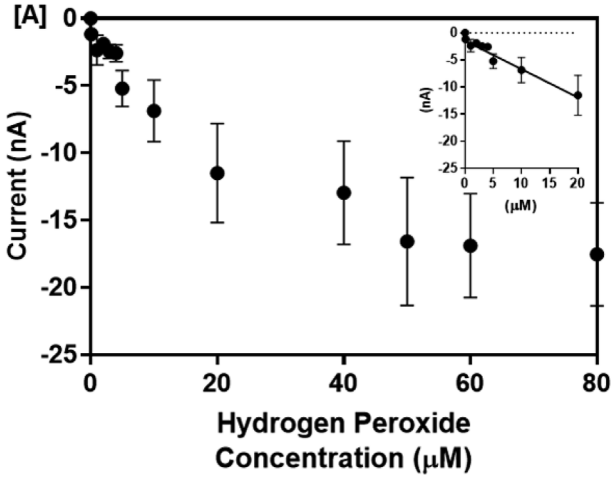

Fig. 2. Calibration curve with varying concentrations of hydrogen peroxide (0.1 μM–80 μM) diluted in PBS. PBS used as a baseline control. Inset: 0–20 μM concentrations that were used to calculate the limit of detection. Points plotted are mean ± 1 SD.

2.11. Analysis

Statistical analysis was conducted with GraphPad Prism 7.

3. Results and discussion

3.1. Determining the limit of detection

Prior to testing the sensors with bacteria, we determined the limit of detection (LoD) of the ITO-SWCNT-Osby sensors for detecting hydrogen peroxide, in order to assess their sensitivity and viability as an intracellular sensor. Considering total intracellular concentrations of ROS are relatively low (< 100 μM)(Huang and Sikes, 2014), and hydrogen peroxide only makes up a fraction of this; our sensor will need to be able to detect low-micromolar concentrations of hydrogen peroxide.

After cleaning the ITO-SWCNT-Osby sensors, chronoamperograms were recorded at a fixed potential of 0.15 V (vs Ag/AgCl) with various concentrations of H_2O_2 using PBS as a blank control. After blank subtraction, current versus concentration was plotted to obtain a linear plot and enable LoD. This can be seen in Fig. 2.

LoD was calculated following the ICH quality control guidelines (ICH, 1994) where from a calibration curve, the standard deviation (SD) of one of the lowest concentrations is used with the fitted slope of the curve. Calculation of LoD is shown in equation (1)

$$LoD = \frac{3.33 \times SD}{slope} \quad (1)$$

Using this equation, the theoretical LoD for the ITO-SWCNTs-Osby sensors was calculated as 368 nM, with the lowest tested concentration being 100 nM. In practice however, a change can easily be identified in current with concentrations as low as 100 nM (see Fig. 2 inset).

Previously our group has conducted preliminary experiments using lipopolysaccharides (LPS) extracted from bacteria. In all previous experiments 1 μg/ml LPS was used (Rawson et al., 2015), LPS concentrations were analysed in relation to the normal growth curve of the bacteria. Fig. 3[A] displays the typical growth curves of *S.minnesota Re595* (left y axis) as measured by its absorption at 600 nm (OD_{600}); and its corresponding endotoxin concentration with time (right y axis). LPS concentration can be approximated from endotoxin concentration as approximately 1 ng/ml of LPS is equivalent to 12 EU/ml (as provided by the supplier). Endotoxin concentrations, and therefore approximate LPS concentrations, were calculated using a commercially available LAL assay kit. Fig. 3[B] shows the endotoxin concentration of the three

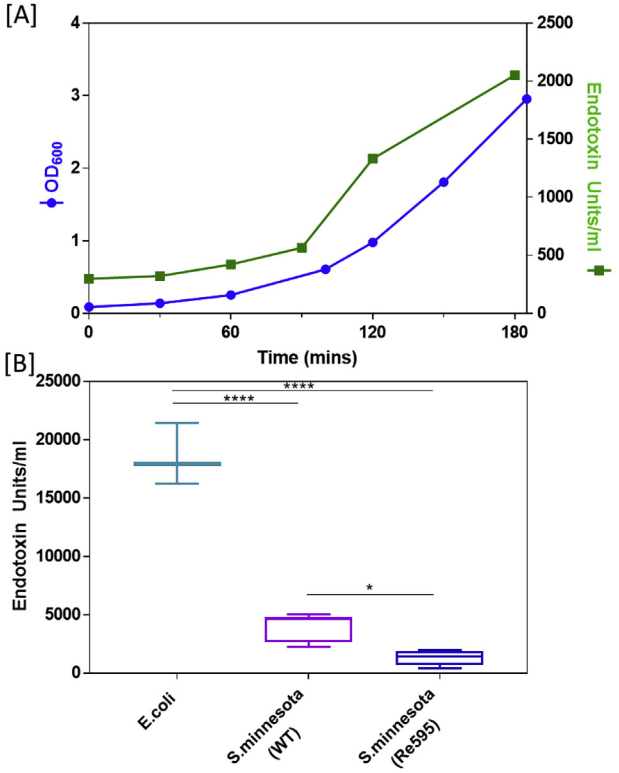

Figure 3. [A] Typical growth curve of *S.minnesota* Re595 (left y axis) up to 2 hours and endotoxin concentration (right y axis, EU/ml.) [B] Box and whiskers plot of endotoxin concentration, as calculated by LAL assay, after bacteria have been growing in suspension for two hours. N = 4. Tested for significance by one-way ANOVA with TUKEY post-test. E.coli vs both *S.minnesota* strains $p < 0.0001$, *S.min*nesota WT vs Re595 $p = 0.0106$.

different bacterial serotypes after two hours of growth in suspension. By this time each bacterial strain is within the early exponential phase of growth.

3.2. Whole bacteria experiments

By two hours of growth in suspension all three bacterial strains have entered their early exponential growth phase and have similar densities (as measured by the OD_{600}, see supporting information S1) though their endotoxin concentrations vary (Figure 3B). The *E.coli* (WT/smooth strain) having a particular high concentration of 18540 EU/ml, when compared to both *S.minnesota* strains which are 3924 EU/ml (WT) and 1332 EU/ml (Re595). Subsequent experiments were conducted using approximately 100 ng/ml (LPS concentration, equal to 1200 EU/ml) of each bacterium to be more comparable to current literature and to not overload the cell with unnecessarily high bacterial concentrations.

The aim of this work, as stated, is to be able to distinguish between different bacterial serotypes based on their current response using our H_2O_2 biosensor. Numerous controls were conducted to ensure we were precisely measuring intracellular H_2O_2. NAC was used as a generic antioxidant to reduce total ROS (Ezerina et al., 2018). Sodium pyruvate is membrane diffusible and acts as a scavenger for hydrogen peroxide (Jagtap et al., 2003); confirming the signal response is a result of change in hydrogen peroxide concentration. TAK-242, a TLR4 inhibitor (Matsunaga et al., 2011), was also used to determine how much of the total response is resultant from the bacterial LPS binding to the TLR4/MD-2 complex. With these controls we were able to ascertain of the total response detected by our ITO-SWCNT-Osby sensor what percentage of this signal is LPS induced, while confirming that we are specifically detecting intracellular H_2O_2.

Hydrogen peroxide response was measured by the change in

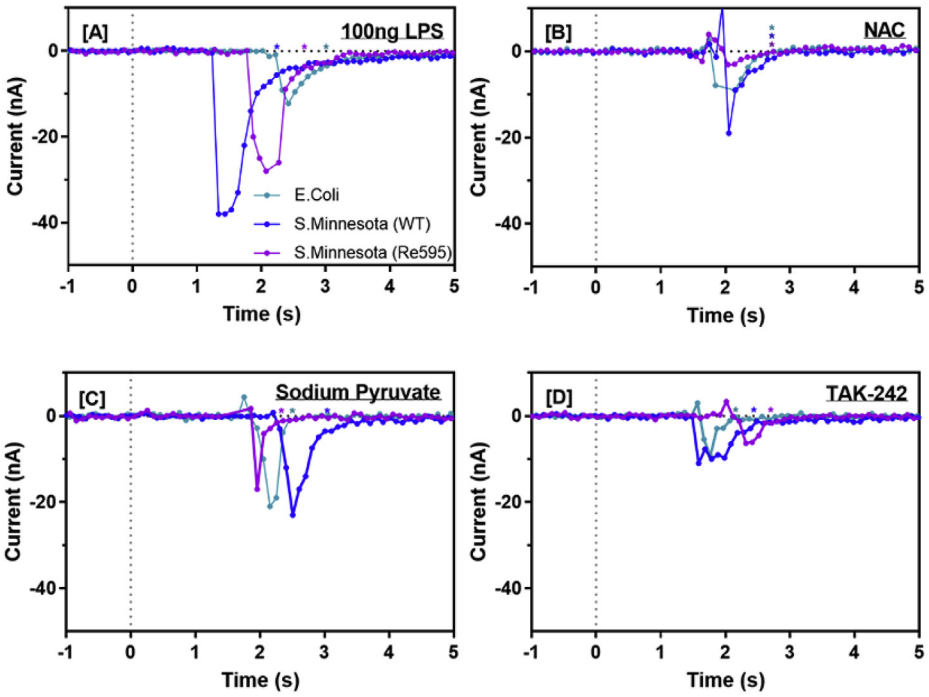

Fig. 4. Typical chronoamperogram responses post bacterial stimulation after baseline subtraction. Time 0 = time at which bacteria is introduced to the solution. [A]-[D] pale blue line represents E.coli, dark blue- *S.minnesota* (WT) and purple is *S.minnesota* (Re595). [A] Bacterial response with no cell treatments, [B] cells pre-treated with NAC, [C] cells pre-treated with sodium pyruvate and [D] cells pre-treated with TAK-242. Scans were baseline corrected pre-time 0. For calculating the average current post-stimulation 100 data points were averaged after the period of diffusion and disturbance of the diffusion layer (indicated by coloured asterisks). (For interpretation of the references to colour in this figure legend, the reader is referred to the Web version of this article.)

current, when macrophage cells were exposed to bacteria by the ITO-SWCNT-Osby sensor. A fixed potential of 0.15 V applied to the sensor, is sufficient for maintaining the osmium in its reduced state, keeping it primed and ready to be oxidised by H_2O_2. An increase in local H_2O_2 concentration will result in an increase in reduction current which is proportional to the concentration change. A baseline is achieved by applying the potential for approximately 10 minutes prior to introducing the bacteria to the electrolyte solution (PBS) and the cells. Typical responses can be seen in Fig. 4.

Bacteria are introduced at '0 s' and a response is consistently seen within 3 seconds. The change in current was measured by averaging the current for 10 s prior to bacterial infection and for 10 s after either the end of measured diffusion or once a new baseline is established. Examples of this are indicated by the asterisks (*) in Fig. 4[A-D]. Controls were performed to confirm our previous report that the sensor was detecting H_2O_2 (Rawson et al., 2015) and that there was no interference from other cellular components. This was based on using an anti-oxidant NAC with cells which reacts with ROS, sodium pyruvate which is well established to enter cells and selectively react with H_2O_2. On addition of sodium pyruvate in LPS stimulated cells the signal is reduced in comparison to LPS only. This indicates that the signal is from H_2O_2 and not interfering species (Fig. 5). If the signal resulted from molecules other than the H_2O_2 then adding sodium pyruvate would not have had an effect as this selectively reacts with H_2O_2. Finally, a TLR-4 inhibitor TAK-242 was used to block the interaction of LPS with macrophages. The hypothesis being that all the above controls would reduce the H_2O_2 signal previously identified to be induced by isolated LPS (Rawson et al., 2015). When cells are pre-treated, as described with either NAC, sodium pyruvate or TAK-242, the change in current is greatly reduced as can be observed. PBS was used as a negative control to see the effect of the disruption of the Nernst diffusion layer by the motion of the pipetting into the electrolyte solution. When PBS is pipetted into the total analyte solution there is a minor positive change in current. With the bacteria, in all cases, there was an increase in the reductive current change which, is indicative of the osmium core being re-reduced after being oxidised by the H_2O_2. When the cells are pre-incubated with NAC this signal becomes positive, comparable to the PBS response (*E.coli* + NAC p = 0.0002***; *S.minnesota* WT + NAC p = 0.0452*; *S.minnesota* Re595 + NAC$^{n.s.}$), providing evidence that the signal is entirely produced from an increase in intracellular ROS. When the cells are pre-incubated with sodium pyruvate however, the majority of the signal is abolished but not to the same level as the PBS control (*E.coli* + sodium pyruvate p = 0.003**; *S.minnesota* WT + sodium pyruvate p = 0.021*; *S.minnesota* Re595 + sodium pyruvate$^{n.s.}$). This shows that the majority, if not all, of the signal produced is a measurement of intracellular hydrogen peroxide. When the TLR4 receptor is inhibited, with TAK-242, and thus the production of LPS induced intracellular ROS inhibited, we get a varied response between the bacterial serotypes (Fig. 5A–C). With both wild-type, smooth bacterial serotypes (*E.coli* and *S.minnesota*) the signal is reduced by approximately 65%. The signal from the rough serotype of *S.minnesota* (Re595) however, is completely abolished and is insignificantly different from the PBS control.

A comparative of the change in current from the three different serotypes can be seen in Fig. 5[D]. The smooth *E.coli* bacteria gave a greater response of −475.3 pA, than the rough *S.minnesota* bacteria of −163.0 pA. Continuing on from this trend the smooth LPS form of *S.minnesota* gave a significantly greater response than its rough counterpart of −770.7 pA. While stability of the sensors have been tested and published previously (Hicks et al., 2017), Fig. 5 also shows the reproducibility of bacterial testing with these biosensors with the standard errors being no larger than 12% of the total signal (*E.coli* = 12%, *S.minnesota* = 10% and *Re595* = 7%). Most importantly, all three serotypes gave significantly different responses from each other. This sensing platform therefore, may be of great use in the future in differentiating between bacterial infections.

Colony forming units per ml (CFU/ml) after two hours of growth were also identified to compare response to bacterial concentration as well as to LPS concentration. The results of these calculations can be seen in Table 1. From this we can see again see that the *S.minnesota* rough LPS gives a lower response per CFU than its smooth (WT) counterpart. However, it seems per CFU the *E.coli* serotype is more pathogenic that the *S.minnesota* WT serotype.

The hypothesis was that different bacteria would give different H_2O_2 responses. We expected that the rough mutant LPS would result in a much higher ROS response based on current literature where rough LPS has been shown to produce a faster and much more concentrated ROS burst (Ruchaud-Sparagano et al., 1998; Beutler et al., 2003).

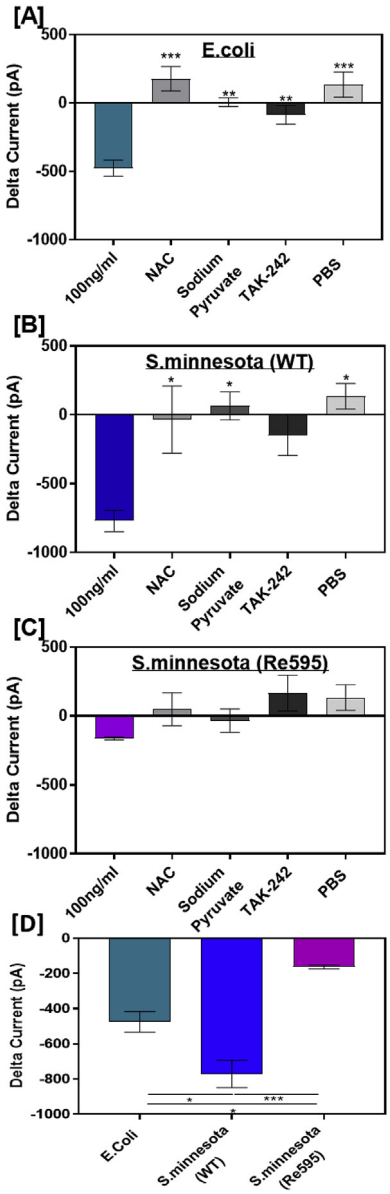

Fig. 5. Bar graph of mean change in current (ΔpA) after bacterial addition; [A] E.coli, [B] *S.minnesota* (WT) and [C] *S.minnesota* (Re595). A-C show comparative between current change with bacterial addition and addition when the cells have been pre-incubated with either NAC, sodium pyruvate or TAK-242. Control of PBS addition is shown in each. Statistical significance was tested with a one-way ANOVA and Tukey post-test. A-C significance is tested vs bacterial 100 ng/ml LPS sample. ($P < 0.05$*, $p < 0.01$**, $p < 0.001$***). N is between 3 and 6 for all samples. [D] Comparative mean change in current after bacterial addition. Significance tested via one-way ANOVA and Tukey post-test. E.coli vs *S.minnesota* WT $p = 0.019$, E.coli vs *S.minnesota* Re595 $p = 0.0146$, *S.minnesota* WT vs Re595 $p = 0.0005$. E.coli $n = 6$, *S.minnesota* WT $n = 5$, *S.minnesota* Re595 $n = 4$.

Rough LPS does not need to be escorted to the TLR4/MD-2 complex via lipid binding protein and CD14 unlike smooth LPS which does (Jiang et al., 2005; Huber et al., 2006). When CD14 is present (as it is in macrophage cells) rough LPS signalling via the TLR4/MD-2 complex is normally increased (Jiang et al., 2005) also. However, we have seen the opposite of this with both WT (smooth) strains resulting in much greater hydrogen peroxide bursts compared to the rough *S.minnesota* strain. As current research has been limited by detection times within minutes rather than seconds, it could be that rough bacteria give a greater response at these longer timescales. The differences in the hydrogen peroxide bursts highlights how dynamic the immune response is to infection and could mean the difference between the cell initiating apoptosis or cell survival via antibacterial measures such as cytokine and caspase production (Brunialti et al., 2007; Aachoui et al., 2013; Rigato and Salomao, 2003; Cohen, 2002).

The data presented here is a noteworthy initial step in designing a test that can distinguish between bacterial infections and finally understanding the complexities of ROS and the innate immune system.

Table 1
Summary data of current response, LPS concentration and CFU/ml; errors shown are ± 1 SEM.

	E.coli	*S.minnesota* (WT)	*S.minnesota* (Re595)
LPS (ng/ml)	1545 ± 126	327 ± 44	111 ± 18
CFU/ml ($\times 10^9$)	1.0 ± 0.05	0.7 ± 0.12	1.3 ± 0.20
ng LPS/CFU ($\times 10^{-7}$)	15	4.9	0.8
100 ng LPS Current Response (pA)	−440 ± 58	−675 ± 77	−163 ± 11
Response per CFU (pA $\times 10^{-6}$)	−5.5	−1.9	−0.25

4. Conclusion

The work presented here has displayed the development and application of an intracellular sensor capable of detecting nanomolar concentrations of hydrogen peroxide. This was utilised in the investigation of the immune response to bacterial infection and successfully detected hydrogen peroxide within three seconds of infection. Such a response has not been measured before due to the limitations of current technology. This detection method of bacteria is however, limited to gram negative bacteria as it is dependent on the interaction between LPS and TLR4. This is also a highly concentration dependent method of identifying bacterial strains and its applicability to real patient samples needs to be investigated further. Specifically, an expanded study of more bacterial strains within complex media such as plasma. Future work would also include investigating the purpose of this initial rapid production of ROS within immune cells. Other than the sensors applicability to bacterial sensing, they will be of great use in many research areas due to the diverse roles ROS and hydrogen peroxide play within cell signalling and disease.

Declaration of interests

The authors declare that they have no known competing financial interests or personal relationships that could have appeared to influence the work reported in this paper.

The authors declare the following financial interests/personal relationships which may be considered as potential competing interests:

CRediT authorship contribution statement

J.M. Hicks: Formal analysis, Writing - original draft. **N. Silman:** Writing - review & editing. **S.K. Jackson:** Writing - review & editing. **J.W. Aylott:** Formal analysis, Writing - review & editing. **F.J. Rawson:** Formal analysis, Writing - review & editing.

Acknowledgements

This work was supported by the Engineering and Physical Research grant number EP/R004072/1 and Biotechnology and Biological Sciences Research Council grant number BB/L017059/1.

Appendix A. Supplementary data

Supplementary data to this article can be found online at https://doi.org/10.1016/j.bios.2019.111430.

References

Aachoui, Y., Leaf, I.A., Hagar, J.A., Fontana, M.F., Campos, C.G., Zak, D.E., Tan, M.H., Cotter, P.A., Vance, R.E., Aderem, A., Miao, E.A., 2013. Caspase-11 protects against bacteria that escape the vacuole. Science 339, 975–978.

Akira, S., Hoshino, K., 2003. Myeloid differentiation factor 88-dependent and -independent pathways in toll-like receptor signaling. J. Infect. Dis. 187, S356–S363.

Asehnoune, K., Strassheim, D., Mitra, S., Kim, J.Y., Abraham, E., 2004. Involvement of reactive oxygen species in Toll-like receptor 4-dependent activation of NF-kappa B. J. Immunol. 172, 2522–2529.

Belluzo, M., Ribone, M., Lagier, C., 2008. Assembling amperometric biosensors for clinical diagnostics. Sensors 8, 1366–1399.

Beutler, B., Hoebe, K., Du, X., Ulevitch, R.J., 2003. How we detect microbes and respond to them: the Toll-like receptors and their transducers. J. Leukoc. Biol. 74, 479–485.

Brandes, R.P., Weissmann, N., Schroder, K., 2014. Nox family NADPH oxidases: molecular mechanisms of activation. Free Radic. Biol. Med. 76, 208–226.

Brunialti, M., Martins, P., Martos, L., Machado, F., Blecher, S., Salomao, R., 2007. Oxidative metabolism and cytokine production are differentially regulated in monocytes from septic patients. Shock 27, 34 34.

Clark Jr., L.C., Clark, E.W., 1987. A personalized history of the Clark oxygen electrode. Int. Anesthesiol. Clin. 25, 1–29.

Cohen, J., 2002. The immunopathogenesis of sepsis. Nature 420, 885–891.

Ezerina, D., Takano, Y., Hanaoka, K., Urano, Y., Dick, T.P., 2018. N-acetyl cysteine functions as a fast-acting antioxidant by triggering intracellular H2S and sulfane sulfur production. Cell Chem. Biol. 25, 447–459 e4.

Gomes, A., Fernandes, E., Lima, J.L., 2005. Fluorescence probes used for detection of reactive oxygen species. J. Biochem. Biophys. Methods 65, 45–80.

Grieshaber, D., MacKenzie, R., Vörös, J., Reimhult, E., 2008. Electrochemical biosensors - sensor principles and architectures. Sensors 8, 1400–1458.

Hicks, J.M., Wong, Z.Y., Scurr, D.J., Silman, N., Jackson, S.K., Mendes, P.M., Aylott, J.W., Rawson, F.J., 2017. Tailoring the electrochemical properties of carbon nanotube modified indium tin oxide via in situ grafting of aryl diazonium. Langmuir 33, 4924–4933.

Huang, B.K., Sikes, H.D., 2014. Quantifying intracellular hydrogen peroxide perturbations in terms of concentration. Redox Biol. 2, 955–962.

Huber, M., Kalis, C., Keck, S., Jiang, Z., Georgel, P., Du, X., Shamel, L., Sovath, S., Mudd, S., Beutler, B., Galanos, C., Freudenberg, M.A., 2006. R-form LPS, the master key to the activation ofTLR4/MD-2-positive cells. Eur. J. Immunol. 36, 701–711.

Hwang, O., 2013. Role of oxidative stress in Parkinson's disease. Exp. Neurol. 22, 11–17.

ICH, 1994. Validation of analytical procedures: text and methodology. In: Quality Guidelines. ICH. http://www.ich.org/products/guidelines/quality/article/quality-guidelines.html.

Jagtap, J.C., Chandele, A., Chopde, B.A., Shastry, P., 2003. Sodium pyruvate protects against H(2)O(2) mediated apoptosis in human neuroblastoma cell line-SK-N-MC. J. Chem. Neuroanat. 26, 109–118.

Jiang, Z., Georgel, P., Du, X., Shamel, L., Sovath, S., Mudd, S., Huber, M., Kalis, C., Keck, S., Galanos, C., Freudenberg, M., Beutler, B., 2005. CD14 is required for MyD88-independent LPS signaling. Nat. Immunol. 6, 565–570.

Kotanen, C.N., Moussy, F.G., Carrara, S., Guiseppi-Elie, A., 2012. Implantable enzyme amperometric biosensors. Biosens. Bioelectron. 35, 14–26.

Leland, C., Clark, J., Wolf, R., Granger, D., Taylor, Z., 1953. Continuous recording of blood oxygen tensions by polarography. J. Appl. Phys. 3, 189–193.

Lennicke, C., Rahn, J., Lichtenfels, R., Wessjohann, L., Seliger, B., 2015. Hydrogen peroxide – production, fate and role in redox signaling of tumor cells. Cell Commun. Signal. 13, 39.

Mateen, S., Moin, S., Khan, A.Q., Zafar, A., Fatima, N., 2016. Increased reactive oxygen species formation and oxidative stress in rheumatoid arthritis. PLoS One 11, e0152925.

Matsukawa, J., Matsuzawa, A., Takeda, K., Ichijo, H., 2004. The ASK1-MAP kinase cascades in mammalian stress response. J. Biochem. 136, 261–265.

Matsunaga, N., Tsuchimori, N., Matsumoto, T., Ii, M., 2011. TAK-242 (resatorvid), a small-molecule inhibitor of Toll-like receptor (TLR) 4 signaling, binds selectively to TLR4 and interferes with interactions between TLR4 and its adaptor molecules. Mol. Pharmacol. 79, 34–41.

Mittal, M., Siddiqui, M.R., Tran, K., Reddy, S.P., Malik, A.B., 2014. Reactive oxygen species in inflammation and tissue injury. Antioxidants Redox Signal. 20, 1126–1167.

Oliveira, Y.P., Pontes-de-Carvalho, L.C., Couto, R.D., Noronha-Dutra, A.A., 2017. Oxidative stress in sepsis. Possible production of free radicals through an erythrocyte-mediated positive feedback mechanism. Braz. J. Infect. Dis. 21, 19–26.

Pacquelet, S., Johnson, J.L., Ellis, B.A., Brzezinska, A.A., Lane, W.S., Munafo, D.B., Catz, S.D., 2007. Cross-talk between IRAK-4 and the NADPH oxidase. Biochem. J. 403, 451–461.

Rawson, F.J., Garrett, D., Downard, A., Baronian, K., 2011. Electron transfer from Proteus vulgaris to a covalently assembled, single walled carbon nanotube electrode functionalised with osmium bipyridine complex: application to a whole cell biosensor. Biosens. Bioelectron. 26, 2383–2389.

Rawson, F.J., Hicks, J., Dodd, N., Abate, W., Garrett, D.J., Yip, N., Fejer, G., Downard, A.J., Baronian, K.H., Jackson, S.K., Mendes, P.M., 2015. Fast, ultrasensitive detection of reactive oxygen species using a carbon nanotube based-electrocatalytic intracellular sensor. ACS Appl. Mater. Interfaces 7, 23527–23537.

Rawson, F.J., Jackson, S.K., Yeung, C.L., Mendes, P.M., 2013. Tailoring 3D single-walled carbon nanotubes anchored to indium tin oxide for natural cellualr upatake and intracellular sensing. Nano Letts. 13, 1.

Rigato, O., Salomao, R., 2003. Impaired production of interferon-gamma and tumor necrosis factor-alpha but not of interleukin 10 in whole blood of patients with sepsis. Shock 19, 113–116.

Ruchaud-Sparagano, M.-H., Ruivenkamp, C.A., Riches, P.L., Poxton, I.R., Dransfield, I., 1998. Differential effects of bacterial lipopolysaccharides upon neutrophil function. FEBS (Fed. Eur. Biochem. Soc.) Lett. 430, 363–369.

Ryan, K.A., Smith Jr., M.F., Sanders, M.K., Ernst, P.B., 2004. Reactive oxygen and nitrogen species differentially regulate Toll-like receptor 4-mediated activation of NF-kappa B and interleukin-8 expression. Infect. Immun. 72, 2123–2130.

Salomao, R., Martins, P.S., Brunialti, M.K., Fernandes Mda, L., Martos, L.S., Mendes, M.E., Gomes, N.E., Rigato, O., 2008. TLR signaling pathway in patients with sepsis. Shock 30 (Suppl. 1), 73–77.

Schulze-Osthoff, K., Los, M., Baeuerle, P.A., 1995. Redox signalling by transcription factors NF-kappa B and AP-1 in lymphocytes. Biochem. Pharmacol. 50, 735–741.

Terada, L.S., 2006. Specificity in reactive oxidant signaling: think globally, act locally. J. Cell Biol. 174, 615–623.

Winterbourn, C.C., 2014. The challenges of using fluorescent probes to detect and quantify specific reactive oxygen species in living cells. Biochim. Biophys. Acta 1840, 730–738.